

DEVELOPING AN INTEGRATED SYSTEM FOR EXTRACTING THE SUB-FIELDS WITHIN AGRICULTURAL PARCELS FROM REMOTE SENSING IMAGES

M.Turker^a and E. H. Kok^b

^a Hacettepe University, Faculty of Engineering, Department of Geodesy and Photogrammetry, 06800 Beytepe, Ankara, Turkey - (mturker@hacettepe.edu.tr)

^b Middle East Technical University, Geodetic and Geographic Information Technologies, 06531 Ankara, Turkey - (emrehkok@gmail.com)

Commission VI, WG VI/4

KEY WORDS: Agriculture, Extraction of Sub-fields, System Development, Perceptual Grouping, SPOT4 and SPOT5 images.

ABSTRACT:

An integrated system was developed to detect sub-fields within agricultural parcels from remote sensing images. The permanent field boundaries are known and stored in a database. The detection of the sub-fields is carried out on field-by-field basis. The fields are selected one-by-one through a database query. The remotely sensed image is filtered using the Canny edge detector. The detected edges are then vectorized to generate the straight line segments. To reduce the number of line segments, a line simplification algorithm is carried out. Next, the line segments are associated with the existing field boundaries using the perceptual grouping rules and the sub-fields are generated. To do that, for each pair of the line segments, the analysis operations are carried out and an iterative decision mechanism is used to modify the line segments when extracting the sub-fields. The approach was implemented in an agricultural area located near Karacabey, Turkey, where majority of the fields are rectangular shaped that affects field-based image segmentation. The data used include SPOT4 and SPOT5 images and existing vector field boundaries. For each image, (i) the first component of the Principle Component Analysis (PCA) bands, and the intensity image of the first three bands ($[\text{Band1} + \text{Band2} + \text{Band3}] / 3$) were used. Of the four segmentations, the SPOT5-PCA image provided the highest accuracy of 83.8%, while the accuracy of the SPOT5-Intensity image (82.6%) was also not significantly different. The accuracies of the SPOT4-PCA and the SPOT4-Intensity images were computed to be 78.8% and 76.2%, respectively. It was observed that the under-segmented fields were slightly more for the SPOT4 images than those obtained for the SPOT5 images.

1. INTRODUCTION

Automatic classification techniques usually operate on per-pixel basis in isolation from other pertinent information. Therefore, per-pixel techniques often yield results with limited reliability. The reliability of image classification can be improved by including apriori knowledge about the contextual relationships of the pixels in the classification process. Agricultural field boundaries integrated with remotely sensed data divide the image into homogeneous units of pixels. For each field, the geometry of the boundaries defines the spatial relations between the pixels contained within, and enables those pixels to be processed in coherence. Final decision on the class assignment of the pixels contained within each field is made based on their coherent processing. This is unlike per-pixel classification where the decision for each pixel is reached independently. Therefore, the conventional per-pixel image classification can be replaced by a classification which operates on field basis.

The logic of a field-based classification in agricultural areas is that the image is divided into homogenous units (fields) using the knowledge of existing permanent field boundaries. These boundaries are defined by the roads, trees, canals, ditches etc. and are expected not to change frequently. Therefore, the permanent field boundaries can be used as apriori information to perform the classification on a field specific manner. Field-based image classification can be carried out at two moments in

the classification procedure: (i) pre-field classification, and (ii) post-field classification. In pre-field classification, the statistical measures such as, the mean, median and mode values, are calculated per-field. Here, the assumption is that each field contains a unique cover type. The pixel values in each field are then replaced with the computed statistical value and the image is classified on a pixel-based manner. In post-field classification, first, a pixel-based classification is carried out. Then, for each field, the frequency of the classified pixels is computed and the majority pixel is assigned as the label of the field. One major problem associated with both field-based classification techniques is that of within field sub-boundaries. Where within field sub-boundaries exist between different crops planted within the field, the entire field can be classified incorrectly. This is particularly important for those areas where the fields are planted with multiple crops. The more the number of fields with multiple crops the less the accuracy achieved using the field-based classification. To avoid the problems caused by this type of misclassification, it becomes necessary therefore to delineate within field sub-boundaries.

In this study we present an integrated system developed to perform within field segmentation for extracting the sub-boundaries within the permanent agricultural fields from remote sensing images. The segmentation procedure is carried out using an edge based methodology within the permanent boundaries of the existing fields, which are available and stored

in a database. The sub-fields that enclose the homogeneous cover types are detected using the perceptual grouping rules. First, the within field edges are detected using the Canny edge detection filter. Then, the detected edges are vectorized to generate the straight line segments. Next, the line segments are reduced by means of applying a line simplification algorithm. Finally, the line segments are associated with the permanent field boundaries using a rule based perceptual grouping procedure.

2. METHODOLOGY

The main steps of the proposed sub-field extraction method are as follows: (i) within field edge detection, (ii) vectorization and line simplification, and (iii) perceptual grouping of the line segments

2.1 Edge Detection

The agricultural fields to be analyzed are selected one by one through a database query. For each field, the coordinates of the vertices are stored as a formatted text file. The vector field boundaries and the raster image are integrated by geometric registration. Therefore, for each field, the raster image falling within the field being considered can be selected and processed individually. The small and thin fields, in which no sub-fields are expected, are excluded from further processing. Simply, if the shape factor, which is computed using the equation 1, and the area of a field fall below the predefined thresholds then, the field is not included in the segmentation process. In figure 1, the image patches of two parcels to be further processed for detecting the within field sub-boundaries are illustrated.

$$SH = \frac{\sqrt{4\pi \times Area}}{Perimeter} \quad (1)$$

where *Area* = the area of the field
Perimeter = the perimeter of the field
SH = shape factor

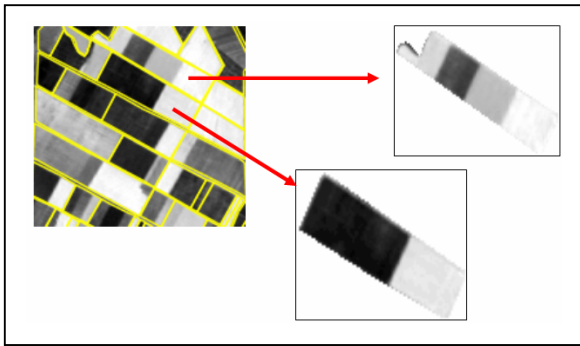


Figure 1. For two parcels, the image patches to be further processed to detect within field sub-boundaries.

Edge detection is a commonly used image processing operation for detecting the rapid variations in the gray level in an image. In the present case, the edges are detected using the Canny edge detector, which provides a connected single line of pixels. The Canny operator requires three parameters; (i) the width of the

Gaussian mask used in the smoothing phase, (ii) the upper threshold, and (iii) the lower threshold used by the tracker. In the present case, while the lower threshold is selected to be very low, the upper threshold is selected to be rather high. The reason for this is that if a narrower threshold range is chosen, the smooth transitions between different crop types may not be detected. On the other hand, removing the noise caused by the over segmentation through applying a contextual based filter on the output appears to be more logical. Therefore, we recommend that over-segmentation should be preferred rather than under-segmentation. In the present case, the threshold values were adaptively determined and used based on the field sizes. After conducting the edge detection operation, a binary image is obtained, in which the white pixels represent the edges while the black pixels represent the others.

Since, for each field, the processings are carried out using the image patch that correspond to the field being considered those pixels falling on the perimeter of the image patch are also detected as the edge pixels. Therefore, the edge pixels that correspond to the perimeter of the field are masked out and excluded from further processing. For field #2140, the image patch, the edge image, and the edge image after the boundary masking procedure is applied are illustrated in figures 2a, b, and c, respectively.

2.2 Vectorization and Line Simplification

Vectorization is a process of detecting the coordinates of the end points of the line segments, which are the candidates for the within field sub-boundaries to be detected from the boundary masked binary image. It is basically a conversion process from raster data set to vector data set. There are several known methods and algorithms to perform such a conversion (Zenko *et al.*, 1996). In the present case, the Suzuki algorithm was used to perform the vectorization process (Suzuki, 1988). First, the thinning of the binary edge image is carried out. Then, a chain graph is constructed using the connected eight edge pixels. Therefore, by associating the connected edge pixels with each other a chain graph is constructed from the edge image. Thus, all the possible lines that may exist within the edge image are extracted through constructing these graphs. Next, the detected edges are converted into the line segments using the vectorization process and, for each line segment, the coordinates of the end points are determined.

After detecting the line segments, a line simplification procedure is carried out. This is necessary to reduce the number of line segments to be further processed and also to retain the longer line segments. To do that the well known Douglas–Peucker algorithm (Hershberger and Snoeyink, 1992), which is a popular method of line simplification, is used. Upon completing the line simplification procedure, the remaining lines to be further processed are grouped according to the connectivity and intersection relations between each other. For field #2140, the vectorized and simplified data set is illustrated in figure 2d.

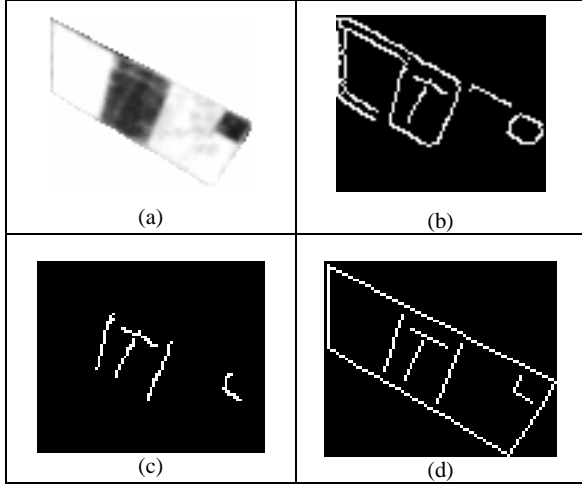


Figure 2. For field #2140, (a) the image patch, (b) the edge image, (c) the boundary masked edge image, and (d) the vectorized and simplified data set

2.3 Perceptual Grouping of the Line Segments

The vectorized and simplified line segments still do not represent the closed regions. Therefore, these unconnected line segments must be further processed to detect the within field sub-boundaries. In order to do that, the vertices of the line segments must be associated both with the existing field boundaries and with the other line segments. This is carried out by means of a rule-based perceptual grouping procedure designed specifically for this study. Simply, the procedure consists of two main steps that are (i) removing the noisy line segments, and (ii) modifying the vertices of the remaining line segments.

In figure 3, the logic of the perceptual grouping is illustrated using a sample field, which contains the line segments to be processed for detecting the within field sub-boundaries. The main input set to be processed consists of the contour lines. A contour line contains a group of the connected line segments. The input set for the sample field given in figure 3 is expressed as;

$$MS = \{ \text{Contour-B, Contour-C, Contour-D, Contour-E, Contour-F, Contour-G, Contour-H} \},$$

e.g: $\text{Contour-E} = ([E1-E2], [E3-E4])$ and Contour-B is the existing field boundary

(2)

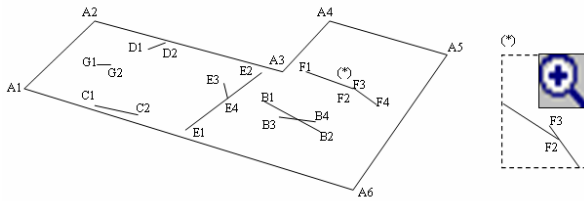


Figure 3. A sample field that contains the detected line segments to be processed for constructing the sub-polygons.

Further, the pairs of the line segments within a contour set and between the contour sets are analyzed and the end points of the line segments are modified (extended and shortened) in order to remove the noisy lines and construct the within field sub-polygons. In addition, the distance, slope, and the possibilities of an intersection between the line segments are computed and analyzed by checking them against the pre-defined threshold values. The parameters used to perform the analyses between the line segments are given in figure 4.

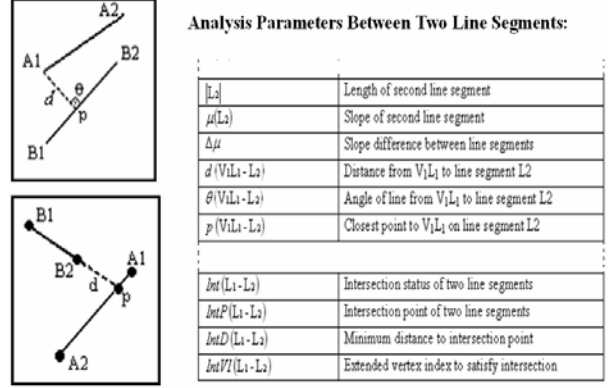


Figure 4. The analysis parameters used to construct the within field sub-polygons.

The analysis parameters are used through a sequential rule-based process. The rules can be summarized as follows:

- Rule 1: In each contour set, remove the overlapping and the intersecting line segments.
- Rule 2: In the main set, remove those line segments that are close to each other.
- Rule 3: Extend the line segment so that it intersects with the existing field boundary.
- Rule 4: Extend the line segments to see if they intersect with each other.
- Rule 5: Remove those line segments that are not extended and shorter than the pre-defined threshold.
- Rule 6: Modify the vertices of the line segments that have open ends by moving the vertex to intersect with the closest line segment.
- Rule 7: Remove the dangling line segments.
- Rule 8: Remove the overlapping line segments and resolve the deviations.

The algorithmic expression of 'Rule 1', which is used to remove the overlapping and the intersecting line segments in each contour set, is expressed as;

$$\forall CS_i \in MS \text{ where } BI(CS_i) = FALSE$$

$$\forall LS_m, LS_n \in CS_i$$

$$\text{analyze}(LS_m, LS_n)$$

$$\text{if } (\Delta\mu \leq \text{ConnectedLineSlopeThreshold})$$

$$\text{if } (d(V_1L_1 - L_2) \leq \text{ConnLineDistThreshold} \text{ and } d(V_2L_1 - L_2) \leq \text{ConnLineDistThreshold})$$

$$\text{remove}(LS_m)$$

$$\text{else if } (d(V_1L_2 - L_1) \leq \text{ConnLineDistThreshold} \text{ and } d(V_2L_2 - L_1) \leq \text{ConnLineDistThreshold})$$

$$\text{remove}(LS_n)$$

(3)

In this rule (Rule 1), in each contour set, except the existing field boundaries (boundary indicator - $BI(CS_i)$ equals to false) each line segment is analyzed against the others contained within the contour set. If the line segment considered is close to and parallel to a longer line segment then, this segment is removed, therefore. For the other rules, the detailed definitions and the algorithmic expressions can be found in K ok (2005). The sequence of the perceptual grouping rules as applied to field #5210 is illustrated in figure 5.

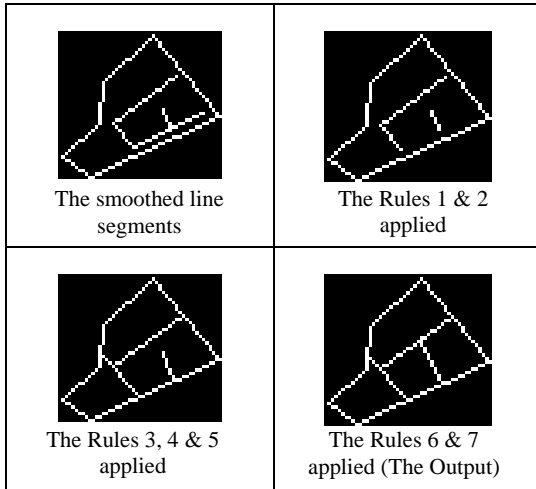


Figure 5. The sequence of the perceptual grouping rules as applied to field #5210.

2.4 Constructing the Sub-Polygons

After detecting, for each line segment, the coordinates of the vertices and finding the connectivity relations between the line segments, the connected line segments are grouped together such that each group defines a disjoint sub-polygon. This is carried out through a chain tree of the line segments, which is constructed using the connectivity relations of the segments and finding the cyclic paths from a point back to itself in the tree. A cyclic path from a point to itself represents a closed polygon. In the tree structure, each node is a vertex of a line segment and this node has child nodes, which can be directly reached from that vertex. Finding all the possible cyclic paths for a vertex means that constructing all the possible polygons that contain this vertex.

After constructing the sub-polygons, it is likely that a number of polygons will have a small size, which is caused by the noisy lines generated through edge detection. Therefore, the small polygons falling below the predefined threshold are merged with the adjacent larger polygons as it is unlikely that the small polygons represent distinct segments of crop types. The merging process is the last step of the proposed segmentation approach and the final output is obtained after this step. In figure 6, the merging of the small fields to the adjacent larger fields are illustrated for fields #2290 and #4402.

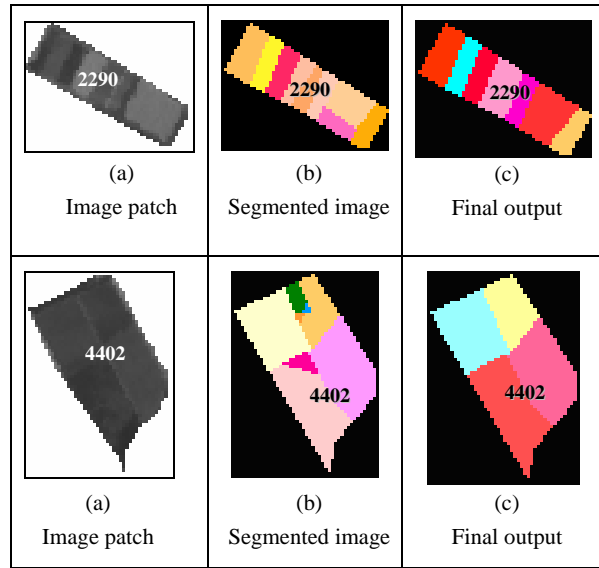


Figure 6. The merging of the small fields to the adjacent larger fields for fields #2290 and #4402.

3. THE IMPLEMENTATION

3.1 Software

To implement the proposed parcel-based image segmentation and sub-boundary extraction procedure, Field-Based Image Segmentation Software (FBISS) was developed using Visual C++ 6.0 and Open Computer Vision (OpenCV, Version 4 Beta) Library, which is a powerful C++ library for the basic image processing operations.

The software includes a number of analysis functions, which provide the capability of performing the whole segmentation process. The following operations can be performed using the developed software:

- Open/Save/Save As/Print Images (several formats)
- Zoom In/Out, Fit to Window, Full Screen Display
- Load Vector File (Formatted Text File)
- Determine Application and Segmentation Parameters
- Perform Segmentation
- Display the Results and Intermediate Outputs
- Compare Between Truth Segments and Results
- Generate Reports of Results (Formatted Text File)
- Merge Segments or Parcels

3.2 Study Area and Data

The study area selected for implementing the concept is an agricultural area located in the Karacabey plain in northwest of Turkey. The size of the area is 4600×7200 m containing 514 fields of various sizes. The area is level plain and largely fertile agricultural with a number of crops under cultivation and several pasture fields for feeding the animals. The crops grown in the region include tomato, corn, pepper, wheat, rice, onion, watermelon, cauliflower, pea and sugar beet. In the region, a land consolidation project was conducted between 1988 and 1992. Therefore, majority of the fields are rectangular shaped, which affects the parcel-based segmentation and the classification procedures. However, despite the land

consolidation project conducted in the region a significant number of small sized fields exist in the study area.

The remote sensing data used include the 20m resolution SPOT4 XS image and the 10m resolution SPOT5 XS image. The existing vector field boundaries, in which the sub-boundary detection procedure to be carried out, were also available. The sub-boundaries within those fields planted with multiple crops were delineated manually by on screen digitization for a previous study conducted in the department (Özdarıcı, 2005). Therefore, this updated field boundary data set was used as the reference to assess the accuracy of the proposed parcel-based segmentation procedure. The SPOT4 Principal Components Analysis (PCA) image with the existing field boundaries overlaid is illustrated in figure 7.

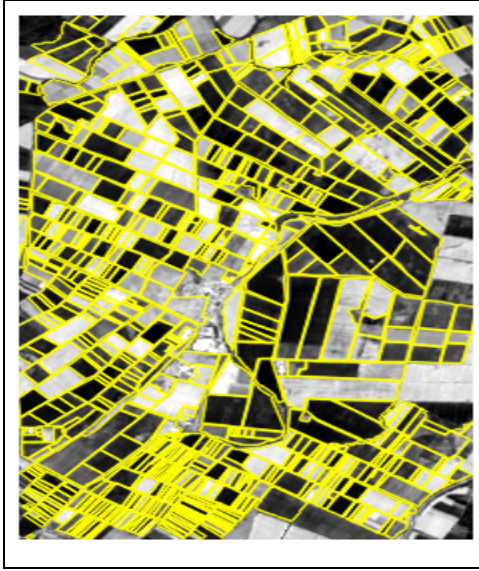


Figure 7. The SPOT4_PCA image with the existing field boundaries overlaid.

We made an assumption that the small and thin fields do not contain multiple crops. Therefore, before starting the segmentation procedure, the small and thin fields were excluded from further processing. It was found that of the total 514 fields, 222 were small and/or thin and therefore, they were not included in the further processing procedures.

Since the segmentation process can be applied on single bands only, the four spectral bands (Green/Red/NIR/SWIR) of the SPOT4 and SPOT5 images were combined using two different methods and two separate single band images were generated for both image data sets. These are;

1. the 1st Components of the Principle Component Analysis bands, (SPOT4_PCA and SPOT5_PCA), and
2. the intensity image - (Green+Red+NIR)/3, (SPOT4_I and SPOT5_I)

3.3 Accuracy Assessment

The accuracy assessment was performed by overlaying the field geometries obtained through the segmentation process (the result segments) with the geometries of the manually digitized field geometries (the truth segments). The match between the two objects M_{ij} can be expressed as a geometrical mean of the

two conditional probabilities of M_i and M_j (Janssen and Molenaar, 1995).

$$\begin{aligned}
 M_{ij} &= \sqrt{(M_i \bullet M_j)} \\
 M_i &= \text{Area}(i \cap j) / \text{Area}(i) \\
 M_j &= \text{Area}(i \cap j) / \text{Area}(j)
 \end{aligned}
 \tag{4}$$

M_{ij} gets a value between 0 and 1. The value of 0 means that there is no matching between the two data sets at all, while the value of 1 indicates a complete match. For each permanent parcel, a mean percentage (MP) was calculated by selecting the overlapping pairs between the manually extracted sub-fields (truth segments) and the result segments. Therefore, for each permanent parcel, the mean of the computed MP values was accepted as the assessed overall accuracy, which is named as Verification Parameter1 - VP1.

Several other parameters are also considered for assessing the results of the segmentation. First, a success criterion is determined by defining a threshold value of 75% for the matching percentage (Janssen and Molenaar, 1995). The truth segments that have a matching percentage with the result segments higher than the predefined threshold are accepted to be successfully detected. The outputs for the other truth segments are considered to be unsuccessful. The ratio of the successfully detected truth segments to all truth segments is calculated and used as another verification parameter, which is named as Verification Parameter2 - (VP2).

In addition, the matching percentage averages are calculated for the successfully detected segments (VP3) and for the unsuccessfully detected segments (VP4). Finally, a quantitative analysis is performed between the result segments and the truth segments by means of measuring the over- and under-segmentations.

3.4 Results and Discussion

The proposed sub-field detection procedure was carried out using each of the four single band images. For a part of the study area, the result (output) segments and these segments superimposed on the SPOT4_PCA band are illustrated in figures 8a and b, respectively.

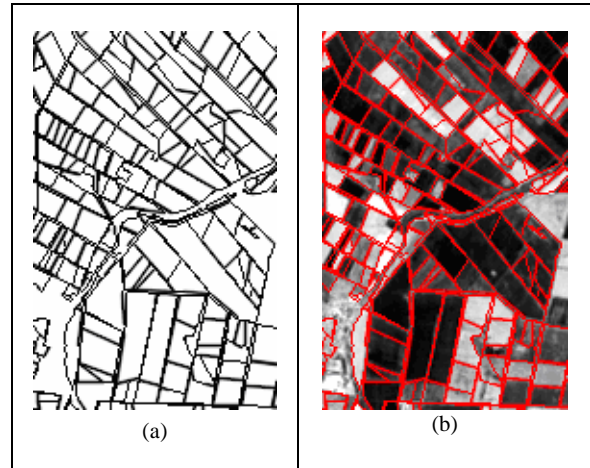


Figure 8. For a part of the study area, (a) the result segments and (b) the result segments superimposed on SPOT4_PCA image.

The quantitative results are summarized in table 1, which contains the number of fields that are over-segmented (OS), under-segmented (US), and equally segmented (ES - number of truth segment = number of result segment for a field) over the processed 292 fields. The geometric errors (GE) for the equally segmented fields are also provided in Table 1. The quantitative results indicate that neither a significant under-segmentation nor a significant over-segmentation is present in the outputs. In the segmentation of the SPOT4 images, the under-segmented fields are found to be slightly more than those obtained for the segmentation of the SPOT5 images.

	US	OS	ES	GE (%)
SPOT5_PCA	52	60	180	3.5
SPOT5_Intensity	62	53	177	2.8
SPOT4_PCA	81	46	165	2.6
SPOT4_Intensity	95	43	154	2.0

Table 1. The Quantitative Results.

The results of the analyses performed based on geometrical relations between the detected and the truth segments are given in table 2, where the overall accuracy (VP1 =83.8 %) is the highest for the SPOT5_PCA image. The values for VP2, which is another accuracy metric, seem to be lower than the overall accuracies. However this parameter must be considered together with VP3 and VP4. The matching percentage averages for the successfully detected truth segments (VP3) are generally very high. This means that the successfully segmented fields have the geometric accuracy of about 95%. Also the unsuccessfully segmented fields have the geometric accuracy of about 50% (VP4), which means that those fields are not completely unsuccessful.

	VP1 (%)	VP2 (%)	VP3 (%)	VP4 (%)
SPOT5_PCA	83.8	70.6	94.6	54.8
SPOT5_Intensity	82.6	67.5	94.6	54.1
SPOT4_PCA	78.8	61.5	94.2	52.1
SPOT4_Intensity	76.2	57.6	93.9	49.3

Table 2. The results based on geometrical analyses between the result segments and the truth segments.

It is evident that a better performance was achieved for extracting the sub-fields through the analyses of the SPOT 5 images although the SPOT5 images have higher resolution than the SPOT 4 images. When the performance of the intensity and the PCA images were compared, it was found that the PCA images, which contain the spectral variability of the all bands, provided slightly better results than the intensity images. It appears that the PCA images contain higher contrast and sharper transitions between the crop fields. Therefore, these might be the reasons for achieving better results from the PCA images.

4. CONCLUSIONS

It was observed that the performance of the proposed parcel-based segmentation technique is strongly dependent on the performance of the edge detection. Better results would be obtained if the Canny edge detector successfully detects the

edges. On the other hand, unsatisfactory results would be obtained if the output of the Canny edge detector contains a large amount of noisy edges or does not contain the proper edges, which might form the missing boundaries.

As a general performance evaluation, the accuracy of the sub-field detection procedure was computed to be $80\% \pm 5\%$, for both the SPOT4 and SPOT 5 images. The results seem to be quite promising. The main reasons for over-segmentation are due to the erroneously detected edges and also the modifications (Rule 4) applied on them. On the other hand, the main reasons for under-segmentation are due to the (i) missing lines that are not able to be detected by the Canny edge detector, (ii) the erroneously deleted line segments through perceptual grouping, and (iii) the erroneously merged sub-fields. In addition, the transformation of the multi-spectral satellite images into a single band image may also cause the loss of information. It is believed that, in some cases, the loss of information might have significant effects on the accuracy of the segmentation procedure.

The accuracy of the proposed parcel-based sub-field detection technique can be further improved. As is well known, the edge detectors are applied on single bands of the images. Therefore, to preserve the whole spectral variability contained by a multi-spectral image, the multi-spectral bands may need to be reduced to a single band. It is recommended that an edge detection technique should be developed that can be applied on multi-band images. In addition, the rules of the perceptual grouping can be improved. The authors believe that the proposed parcel-based sub-field detection strategy is a starting point for the development of a high performance field-based image analysis operation that includes both the segmentation and the classification procedures.

References

- Hershberger, J., and Snoeyink, J. 1992. Speeding Up the Douglas-Peucker Line Simplification Algorithm. In *Proceedings, 5th International Symposium Spatial Data Handling*, p. 134-143.
- Janssen, L. L. F. and Molenaar M. 1995. Terrain Objects, Their Dynamics, and Their Monitoring by The Integration of GIS and Remote Sensing, *IEEE Transactions On Geoscience and Remote Sensing*, 33(3): 749-758.
- Kök, E. H. 2005. Developing An Integrated System For Semi-Automated Segmentation of Remotely Sensed Imagery, M.Sc. Thesis, Geodetic and Geographic Information Technologies (GGIT), Middle East Technical University, Turkey, 146 pages.
- Özdarıcı, A. 2005. Accuracy Assessment of the Field-Based Classification Using the Different Spatial Resolution Images, M.Sc. Thesis, Geodetic and Geographic Information Technologies (GGIT), Middle East Technical University, Turkey, 113 pages.
- Suzuki, S. 1988. Graph-based Vectorization Method for Line Patterns. In: *Computer Society Conference on Computer Vision and Pattern Recognition*, Ann Arbor, MI, June 5-9 pp. 616-621.
- Zenzo, S. D., L. Cinque, and S. Levialdi. 1996. Run-Based Algorithms for Binary Image Analysis and Processing. *IEEE Transactions on Pattern Analysis and Machine Intelligence*, 18(1): 83-89.